Desalination and Water Treatment
www.deswater.com

13 (2010) 290–302
January

1944-3994/1944-3986 © 2010 Desalination Publications. All rights reserved
doi: 10.5004/dwt.2010.1037

A preliminary study of particle dynamics in the water column of Saronikos Gulf, Greece, by using Th-234/U-238 disequilibrium approach

N. Evangeliou[a,b*], H. Florou[a], M. Scoullos[b]

[a]N.C.S.R. 'Demokritos', Institute of Nuclear Technology-Radiation Protection, Environmental Radioactivity Laboratory, 15310, Agia Paraskevi, Athens, Greece
Tel.: +30-210-6503812, Fax.: +30-210-6503050; email: nevag@ipta.demokritos.gr
[b]National and Kapodistrian University of Athens, Department of Chemistry, Laboratory of Environmental Chemistry, Panepistimiopolis, Zografou, 157 71, Athens, Greece

Received 26 February 2009; accepted 9 July 2009

ABSTRACT

In the present study the particle export flux in the water column of 3 sampling stations (one of them near the pipeline outfall of the Waste Water Treatment Plant—WWTP of Psitalia) in the Eastern Saronikos gulf, Central Greece, is investigated based on the disequilibrium ratio of ^{234}Th with its parent ^{238}U. This approach is based on direct measurements of the activity concentrations of ^{234}Th and calculated ones of ^{238}U from the respective salinity measurements. From the derived results, the values of the activity concentrations of particulate and dissolved fraction of ^{234}Th in the surface layer of the studied area range from 2.7 ± 1.4 to 3.8 ± 1.8 Bq m^{-3} and 13.2 ± 1.4 to 28.2 ± 1.9 Bq m^{-3} respectively, which educe fluctuation according to the station environmental features. Regarding the vertical distribution of radionuclides, the observed profile curves from the 3 sampling stations follow the same pattern of dispersion in the water column. However, the calculated export flux (sinking rate) of particles associated with ^{234}Th results to a wide range of values depending on the sampling station. From the calculated residence times in the 3 stations, the station near the WWTP shows the longer residence time for the dissolved fraction, which is attributed to the sewage outflow. Besides, total suspended matter (TSM) and dissolved organic carbon (DOC) have been analyzed in the samples and the correlation coefficients with the particulate and dissolved ^{234}Th have been calculated on the basis of the relation of ^{234}Th cycling with particulate matter and organic substances.

Keywords: Thorium-234; Uranium-238; Eastern Saronikos Gulf; Sinking particles; Export flux; Mean residence times; Oceanography

1. Introduction

Since the first reported measurements of thorium-234 (^{234}Th) in the ocean by Bhat et al. [1], decreases in ^{234}Th activities between open ocean and coastal waters indicated that ^{234}Th activity distributions were strongly influenced by the marine particle cycle. This prompted the use of ^{234}Th as a new in situ tracer of oceanic scavenging, a term used to describe the complex processes related to the association of particle reactive elements with particle surfaces and their removal in the marine environment [2]. Thorium is considered as suitable for tracing processes occurring over timescale of days to weeks [3,4], due to its high

---

*Corresponding author

Presented at the AQUA 2008 International Conference on Water Science and Technology-Integrated Water Resources Management, 16–19 October 2008, Athens Greece.

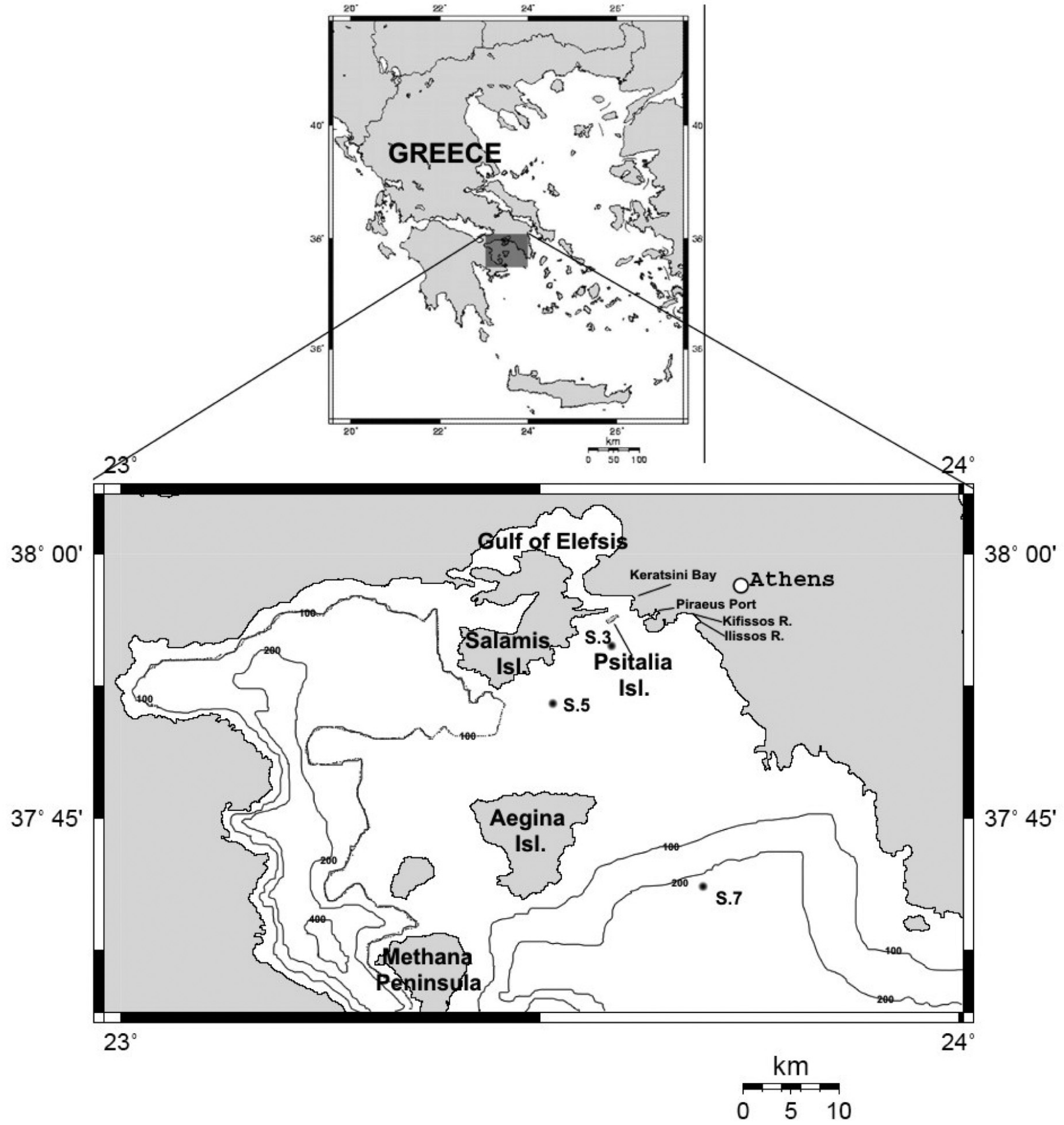

Fig. 1. The area of interest (Saronikos Gulf, Greece).

particle reactivity and its relatively short half-life ($t_{1/2} = 24.1$ days). Using simple activity balance equations [5–7], the ratio of the particle reactive radionuclide ^{234}Th to its soluble and long lived parent, ^{238}U, can be used to quantify the rate of uptake of ^{234}Th onto particles and their export flux out of the surface layer. A larger disequilibrium in total activities (^{234}Th:^{238}U activity ratios) usually reflects a higher export flux [8].

In coastal environments, the primary sources of these radionuclides include, (i) radiogenic production from the parent, (ii) direct atmospheric deposition, (iii) erosional input in the watershed through the discharge of streams and rivers, and deposit through physical exchange processes [9]. The aims of the present work are (i) to address the flux of particles (>0.6 μm) in the water column using ^{234}Th and its radiogenic production equilibrium with its parent ^{238}U as a tool, for investigating the controlling and removal of particle-reactive ^{234}Th in the Eastern Saronikos Gulf (Fig. 1), as well as the importance of the total suspended matter (TSM) in these fluxes; (ii) to determine the residence times of dissolved and particulate fraction of ^{234}Th and

Table 1
Physicochemical characteristics, TSM and DOC concentrations during winter 2007 in the Eastern Saronikos Gulf

Station	Co-ordinates	Depth (m)	Salinity (‰)	Temperature (°C)	pH	Density (kg m^{-3})	TSM (μg L^{-1})	DOC (μmol C L^{-1})
S.3	N37 55.108	0	36.7	14.6	8.66	1,025.29	121	126
	E23 35.294	15	36.4	14.5	8.85	1,026.05	308	272
		60	33.1	14.8	8.60	1,027.02	182	230
S.5	N37 51.287	0	38.1	14.3	8.06	1,028.52	239	124
	E23 33.372	35	37.9	13.5	8.03	1,028.69	294	118
		90	38.4	12.5	8.66	1,029.13	457	202
S.7	N37 42.232	0	38.4	14.4	8.87	1,028.73	631	109
	E23 38.625	50	38.1	13.7	8.68	1,028.81	136	116
		100	37.7	12.8	8.01	1,028.75	223	146
		200	36.5	11.9	8.15	1,028.23	173	370

how they vary with TSM. Besides, as thorium is known to make binds with the dissolved organic ligands, an additional aim of the study is (iii) to investigate the correlation of dissolved ^{234}Th with dissolved organic carbon (DOC), as an indication of the role of ^{234} Th to the organic pollution inventory of the area, in terms of pollutant source and pathway; (iv) to estimate the distribution coefficients (K_d) of ^{234}Th in several depths of the water column and (v) to verify how the specific activity of ^{234}Th vary with depth, as an indication of potential remineralization.

2. The region of interest

The present study has been carried out in the eastern part of the Saronikos Gulf, Greece (Fig. 1). The Saronikos Gulf is typical of many semi-enclosed seas in the Mediterranean and presents two sections, the eastern and the western ones, separated by Aegina Island (Fig. 1). The eastern section, characterized by the Athens metropolitan area, has relatively uniform depth topography, with a maximum depth of 200 m to the south-east of Aegina to 90 m between Aegina and Vouliagmeni. The main body of the eastern basin has depths between 70 and 90 m. The western part of the Saronikos is deeper. From the west of Salamis the basin is 130 m deep and connects to the south with over 400 m maximum depth in the west of the Methana peninsula. At the north end of the Gulf lays Elefsis Bay with maximum depth of about 30 m. The bay is joined to the Gulf by two narrow and shallow channels. The eastern connection, with a dredged channel 11 m deep, communicates with the Keratsini Bay. Depths in Keratsini area are between 25 and 35 m, increasing towards the Saronikos Gulf. Piraeus Port, which is one of the greatest in the Mediterranean Sea, is located about 1 km southern of the eastern channel. The Saronikos Gulf is mainly polluted from the Wastewater Treatment Plant of Psitalia (WWTP), located in a small island near the Piraeus harbour and Keratsini Bay, which discharges pre-treated domestic wastes of Athens (whose population reaches over 4,000,000 inhabitants). Significant amounts of nutrients are also introduced in the form of industrial effluents directly into Elefsis Bay as along the bay more than 30 industries are located (oil refineries, steel mills, shipyards, etc.) [10–12]. In the main Saronikos Gulf the effect of WWTP outflows is evident, as a plume of nutrient-rich water extends about 20 km south of Salamis Island [10].

3. Materials and methods

A suite of samples for 3 vertical profiles of 3 stations (S.3, S.5 and S.7), with final depths of 65, 97 and 220 m, respectively, in the Eastern Saronikos Gulf were collected (Fig. 1) during one cruise at February 2007. Sample locations, water column depths, seawater temperatures, pH, salinities, calculated densities and activity concentrations of particulate and dissolved ^{234}Th, as well as salinity calculated ^{238}U are given in Table 1. Temperature, salinity and pH were determined by an in situ CTD, model YSI 53.

3.1. Particulate and dissolved ^{234}Th sampling

A high volume in situ pump (manufactured by Challenger Oceanic Systems and Services, COSS, UK) was deployed in every selected depth of the tree station. Seawater was directly pumped through a manifold consisting of one disc pre-filter and two MnO_2-impregnated cartridges (see, 3.2. Impregnation of MnO_2 cartridges) connected in series and finally through a flow meter to record the volume of the water filtered. Sample volumes of 500–1,000 L were processed at flow rates of 0.3–1.0 $m^3 h^{-1}$. The accuracy of the flow meter is $\pm 2\%$, operating in a range 22.7–2,730 L per hour [13].

The in situ pump operationally separate dissolved and suspended particulate phases via filtration through a pre-cleaned, pre-combusted Whatman GF/A disc filter (pore size of 0.6 μm, diameter of 142 mm). It has been found that these filters are easy to handle and they have a high loading capacity and a very low radionuclide blank [14,15].

3.2. Impregnation of MnO_2 cartridges

Cotton wound cartridge filters (25 cm long and 1 μm pore size) were used in the impregnation procedure. Impregnation was obtained by circulating water suspension of $KMnO_4$ and $MnCl_2 \cdot 4H_2O$ in a closed loop, employing a small pump and the filter to be impregnated. The filters collected the slurry precipitate formed. When the circulating solution was clear, the impregnated filters were removed and dried in an oven at 60–80 °C for 24 h and packed for the sampling. It is important to adjust pH to 8–9 with 1 N NaOH. This is crucial, as earlier studies showed that MnO_2 prepared at pH 0.5 (the final pH of the reaction without pH adjustment) is an inefficient adsorber of various transuranics [14,15].

3.3. Thorium-234 treatment, measurements and analysis

After sampling, the filters were transferred to the laboratory. The disc filters were air dried, rinsed with distilled water to remove the residual salts and directly measured by gamma spectrometry after transfer in a measurement pot (radius 7.1 cm and height 1.0 cm). The cartridges were dried and ashed in ovens at 350 °C. The remaining ash was transferred into special measurement pots (radius 3.4 cm and height 2.0 cm) for gamma spectrometry measurements.

The measurements were carried out in a gamma spectrometry system comprised of a high-purity Germanium detector (*Canberra Coaxial HpGe Detector System*) with a relative efficiency of 90% and resolution of 2.1 keV (at 1.33 MeV photopeak of ^{60}Co). The HpGe detector is connected to a multi-channel analyzer and the whole system is controlled using specialized software (*Canberra Genie 2000*).

The energy calibration is generally performed using standard active sources of ^{22}Na, ^{54}Mn, ^{57}Co, ^{60}Co, ^{109}Cd, ^{133}Ba, ^{137}Cs, ^{241}Am. In this case ^{241}Am and ^{60}Co were used for energy calibration in a range of 2,000 keV in 8,000 channels (0.25 keV/ch). The duration of each measurement was about 7×10^4 s usually overnight. The detector's efficiency is usually calculated (in connection with energy) using standard active source of ^{226}Ra (standard sources' activity was 240 Bq) in the same geometry with the measurement pot. However, in the present study a mixed standard solution of ^{241}Am, ^{109}Cd, ^{139}Ce, ^{57}Co, ^{60}Co, ^{137}Cs, ^{203}Hg, ^{113}Sn, ^{85}Sr, ^{88}Y of total activity of 5,202 Bq was used for efficiency calibration, as it produces more photopeaks in lower energies of the spectrum.

Once the seawater sample is filtered, it is passed sequentially through two cartridge filters that have been impregnated with MnO_2 (see, 3.2. Impregnation of MnO_2 cartridges). It has been previously shown that dissolved thorium is efficiently extracted from seawater by these cartridges [15]. The collection efficiency for each sample can be calculated from the pair of MnO_2 cartridges by the equation:

$$A(^{234}\mathrm{Th}) = \frac{A_1}{E} = \frac{A_1}{1 - \frac{A_2}{A_1}}$$

where A_1 and A_2 are the ^{234}Th activities (decay corrected to the date of sampling) of the first and second MnO_2 cartridge, respectively and E is the collection efficiency [16]. The uncertainties for ^{234}Th activities in the first and the second filter (A_1, A_2) are 1σ values derived from counting statistics (typical counting statistics errors: 0.26 ± 0.01%). The final uncertainty of $A(^{234}\mathrm{Th})$ has been estimated by uncertainty propagation.

3.4. Uranium-238 derived from the salinity

Uranium-238 was calculated via its proportionality with salinity. Typically, the relationship derived by Chen et al. [17] is used in open ocean studies. However, Mediterranean waters are generally of higher salinity than the open Atlantic and Pacific waters, for which this relationship was obtained. It has been found that ^{238}U concentrations in the Mediterranean are enhanced, relative to the U-salinity relationship of Chen et al. [17], due to phosphate fertiliser run-off into the enclosed basins [18]. However, a recent work has compared the Mediterranean with Atlantic and Pacific waters, finding no significant difference in their U-salinity relationship [19]. Although ^{238}U can deviate from conservative behavior in some coastal areas [20–22], this deviation occurs usually where either freshwater or reducing conditions dominate. The salinity ranges observed (33.1–38.1) indicate that freshwater has minor influence on the study area. Therefore, ^{238}U concentrations were derived from the following equation reported by Delanghe et al. [19] for similar salinities.

$$\text{U-238(dpmL}^{-1}) = (0.07065 \pm 0.00146) \times \text{salinity (psu)}$$

or

$$\text{U-238(Bq m}^{-3}) = (1.1775 \pm 0.0243) \times \text{salinity (psu)}$$

3.5. Sampling for TSM and DOC analyses

Samples for the determination of the TSM were collected after the deployment of the high volume pumps. The same pre-combusted, pre-weighted disc filters used for scavenging particulate ^{234}Th (Whatman GF/A filter with pore size of 0.6 μm and diameter of 142 mm) were subsequently rinsed with distilled water to remove residual salts, they air dried, and then weighed in a microbalance Sartorius BP 211 D. The percentage uncertainty of the microbalance is less than 1.

Trapped seawater, inside the cartridge housings of the high volume pump, was collected in order to determine organic carbon content. Since the pumping system is isolated from the environment and considering that the trapped seawater has been already filtered thought 0.6 μm GF/A disc filter, the organic carbon content corresponds to the DOC content. The later was determined by a TOC SHIMADZU analyzer 5000A (percentage uncertainty less than 1), with the method reported by Sigimura and Suzuki [23] and Cauwet [24].

3.6. One dimensional box model applied to ^{234}Th

The general formulation of ^{234}Th activity in the one box model is the result of a balance between continuous production from ^{238}U, radioactive decay of ^{234}Th, removal onto rapidly sinking particles, and transport into or out of the box by advection and diffusion. The temporal change in total ^{234}Th is expressed by:

$$\frac{\partial A^{t}_{\mathrm{Th}}}{\partial t} = \lambda_{\mathrm{Th}} A_{\mathrm{U}} - \lambda_{\mathrm{Th}} A_{\mathrm{Th}} - P_{\mathrm{Th}} + V \qquad (1)$$

where A_{U} and A_{Th} are the ^{238}U and the total ^{234}Th activities (expressed in Bq m^{-3}), respectively, λ_{Th} is the decay constant of ^{234}Th (=0.02876 d^{-1}), P_{Th} (expressed in Bq m^{-3} d^{-1}) is the removal flux of particulate ^{234}Th, and V is the sum of the advective and diffusive fluxes.

The key assumptions of this model are that: (i) steady-state conditions prevail, which means that ^{234}Th activities and removal rates (J_{Th} and P_{Th}) are essentially constant with respect to the ^{234}Th decay constant; (ii) horizontal and vertical advection and diffusion of ^{234}Th are negligible ($V = 0$); and (iii) scavenging of ^{234}Th is irreversible.

Steady-state dynamics are assumed frequently in ^{234}Th/^{238}U disequilibrium studies, in both coastal and open ocean studies [5,6,25,26]. A series of studies have compared steady-state and non steady state models in coastal waters. These have found no significant differences between the ^{234}Th residence times derived by the two models [21,27–29].

The second assumption is that advection and diffusion of ^{234}Th are negligible, horizontally and vertically, as well. Although ^{234}Th diffusion is not significant, several studies have shown advection to contribute to the observed ^{234}Th profiles. For example, in the open ocean upwelling systems can result in significant vertical advection [30,31]. In coastal and continental shelf environments, horizontal advection is more likely to be significant. Several studies have demonstrated important horizontal advection contributions, when ^{234}Th/^{238}U disequilibrium is used to determine fluxes from surface waters [32,33].

The final assumption, irreversible scavenging of ^{234}Th, is valid in coastal waters, given the high K_d for ^{234}Th observed in numerous studies [21,27].

Thus, Eq. (1) is simplified into:

$$P_{\mathrm{Th}} = \lambda_{\mathrm{Th}}(A_{\mathrm{U}} - A_{\mathrm{Th}}) \qquad (2)$$

This formulation of ^{234}Th flux (Eq. 2) is by far the most commonly used model in ^{234}Th export studies, due to its simplicity and ease of application (only total ^{234}Th need be measured) [7].

Since the supply of ^{234}Th is through the decay of ^{238}U, then the removal from the dissolved phase is via either scavenging onto particles or radioactive decay:

$$J_{\mathrm{Th}} = A_{\mathrm{U}}\lambda_{\mathrm{Th}} - A^{\mathrm{d}}_{\mathrm{Th}}\lambda_{\mathrm{Th}} \qquad (3)$$

where J_{Th} is the rate of scavenging of dissolved ^{234}Th onto the particulate phase; A_{U} is the activity of ^{238}U; λ_{Th} is the decay constant for ^{234}Th; and $A_{\mathrm{Th}}{}^{\mathrm{d}}$ is the activity of dissolved ^{234}Th. Similarly, removal from the particulate phase is via radioactive decay or sinking of the particles:

$$P_{\mathrm{Th}} = J_{\mathrm{Th}} - A^{\mathrm{p}}_{\mathrm{Th}}\lambda_{\mathrm{Th}} \qquad (4)$$

where P_{Th} is the rate at which particulate ^{234}Th is lost from the water column via sinking or grazing; J_{Th} is the rate of supply of particulate ^{234}Th via scavenging; $A_{\mathrm{Th}}{}^{\mathrm{P}}$ is the activity of particulate ^{234}Th; and $A_{\mathrm{Th}}{}^{\mathrm{P}}$ λ_{Th} is the rate at which particulate ^{234}Th is lost due to radioactive decay.

Since $\mathrm{J_{Th}}$ and $\mathrm{P_{Th}}$ represent the non-radioactive removal rates for dissolved and particulate ^{234}Th, mean residence times can be defined for both the dissolved (t_{d}) and particulate (t_{p}) phases:

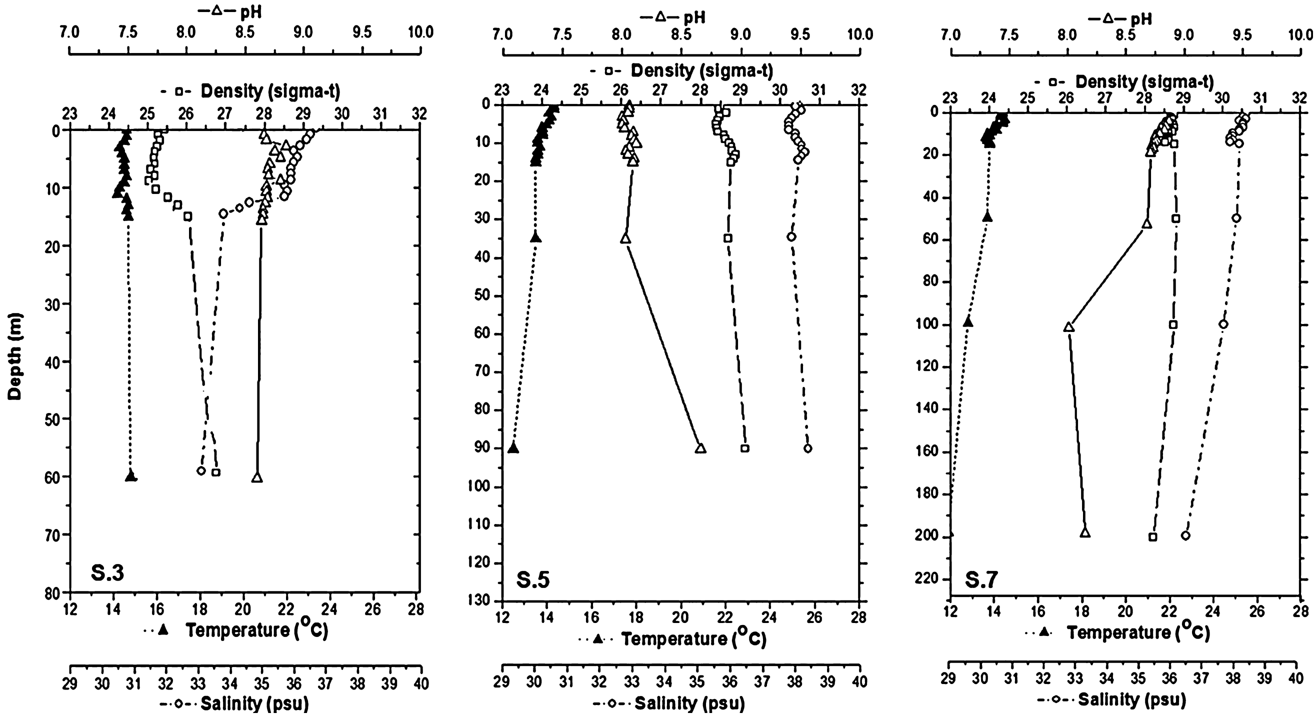

Fig. 2. Vertical profiles of salinity (○), pH (△), temperature (▲) and density (□) in Eastern Saronikos.

$$\tau_d = \frac{A^d_{Th}}{J_{Th}}$$

and $\tau_p = \frac{A^p_{Th}}{P_{Th}}$,

where using Eqs. 3 and 4 becomes:

$$\tau_d = \frac{A^d_{Th}}{(A_U - A^d_{Th})\lambda_{Th}} \tag{5}$$

and

$$\tau_p = \frac{A^p_{Th}}{\left[\left(A_U - A^d_{Th}\right) - A^p_{Th}\right]\lambda_{Th}} \tag{6}$$

The inverse of Eqs. 5 and 6 [34] are the scavenging and removal rates, respectively:

$$\lambda_d = \frac{1}{\tau_d} \tag{7}$$

and

$$\lambda_p = \frac{1}{\tau_p} \tag{8}$$

4. Results and discussion

4.1. Physicochemical characteristics, TSM and DOC concentrations

Station number, sampling depth, salinity, temperature, pH and density values together with TSM and DOC concentrations are given in Table 1 for winter 2007. In order to obtain a more detail view about the characteristics of the water column in the sampling stations, physicochemical parameters are plotted against depth (Fig. 2), as well as TSM and DOC values (Figs. 3 and 4, respectively).

As one can observe, during winter the water column is generally homogenous. A small abnormality is found in the station S.3, as this station is located near the WWTP of Psitalia pipelines. These pipelines outflow low saline, first and second stage treated waste waters in approximately 65 m depth. This fact results in a rapid decrease of salinity in the area with a characteristic halocline near 15 m depth, even though the sampling took place during winter (Fig. 2).

The TSM concentrations vary between 121 and 631 μg L^{-1} in winter depending on depth (Table 1 and Fig. 3). The values are equal to those reported by Krasakopoulou and Karageorgis [35] for the same area. Since S.3 and S.5 are considered as coastal stations and S.7 as open sea one, one might expect elevated values

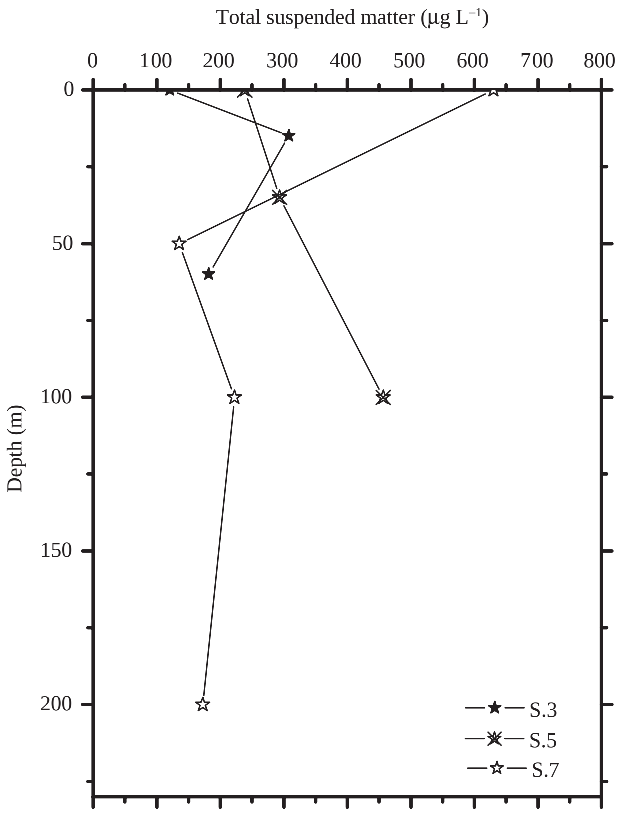

Fig. 3. Vertical profiles of TSM concentrations in S.3, S.5 and S.7 of Eastern Saronikos Gulf.

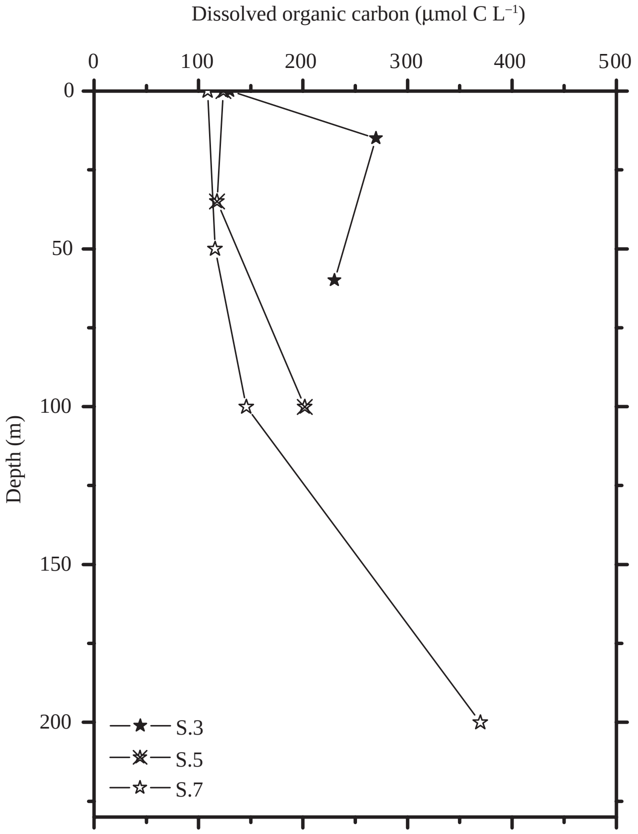

Fig. 4. Vertical profiles of DOC concentrations in S.3, S.5 and S.7 of Eastern Saronikos Gulf.

in coastal stations. However, comparable values are found in every station. This is attributed to the particle sources of each station. Station S.3, for example, is located near the WWTP pipelines, and this is a considerable source of particles near the final depth (65 m). Besides, S.5 is next to the ship anchorage area of the Piraeus Port and this is the main reason that TSM is increased in greater layers. Finally, S.7 is adjacent to the ship traffic of the Piraeus Port and thus surface TSM is increased with maximum to be 631 μg L^{-1}, which is probably caused by weather or anthropogenic processes. For example, trawling or storm events lead to an increase of surface TSM [36].

TSM values increase with depth in two of three stations in winter (Fig. 3). This is attributed to the weather and anthropogenic processes mentioned that affect mostly the surface area. The fact that TSM is enhanced in the stations mentioned is in good agreement with those reported by Krasakopoulou and Karageorgis [35]. This pattern suggests that the primary source of terrigenous particulate matter in the Saronikos Gulf is the WWTP, the Athens metropolitan area and neighbouring, which is highly populated and other industrialised regions (e.g. the coast of Elefsis Bay). Except from atmospheric inputs, the transport pathway of terrigenous material into the gulf is small rivers and ephemeral streams. For example, the rivers Kifissos and Ilissos which discharge near Piraeus (Fig. 1) supply the area with terrigenous particulate matter. Another explanation for determining high TSM concentrations in deeper layers could be possible re-suspension, but this issue is examined using the disequilibrium between total ^{234}Th and ^{238}U.

DOC concentrations are illustrated in Fig. 4 and Table 1, ranging between 109 and 370 μmol C L^{-1} depending on depth. These concentrations are higher than the reported ones for the Mediterranean Sea. For example, in coastal waters of the Gulf of Lions and the Rhone estuary, Cauwet et al. [37] reported DOC values ranging from 58 to 183 μmol C L^{-1}. For the offshore waters of the NW Mediterranean, Cauwet et al. [38] reported DOC concentrations which do not exceed 250 μmol C L^{-1}, and Copin-Montegut and Avril [39] found maximum DOC concentrations at 100 μmol C L^{-1}. Miller et al. [40] in NE Atlantic found DOC concentrations between 150 and 200 μmol C L^{-1}. On the other hand, they are also comparable with those reported by Zeri and Krasakopoulou [41] for the same area.

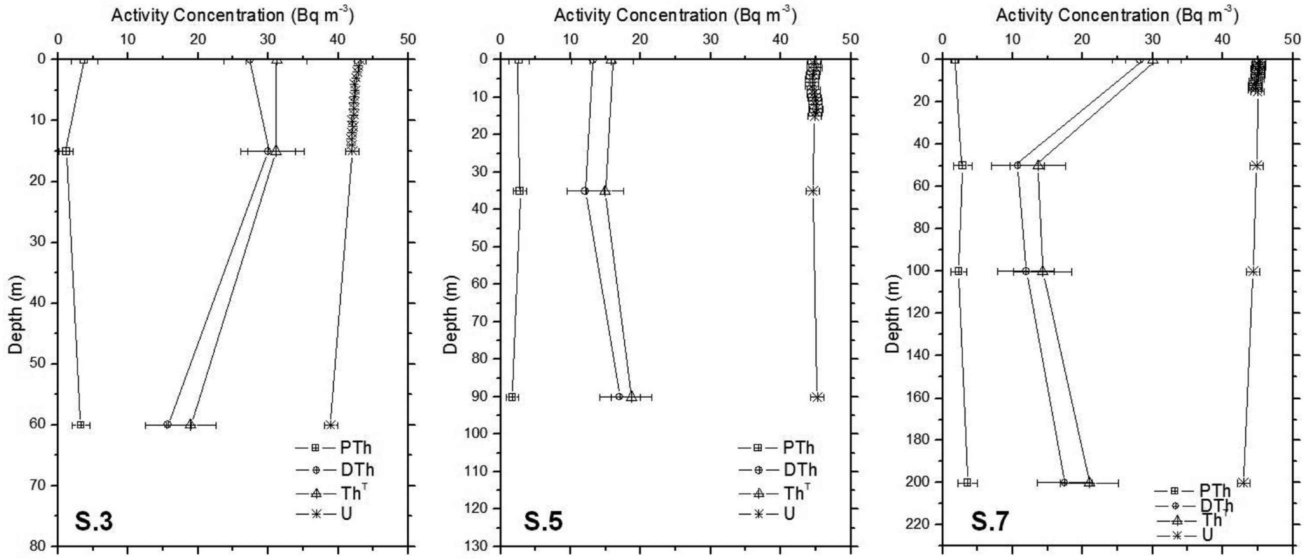

Fig. 5. Vertical profiles of, particulate (P_{Th}, ⊞), dissolved (D_{Th}, ⊕), total ^{234}Th (Th^T, Δ) and ^{238}U (✱) during winter 2007 in the Eastern Saronikos Gulf, Greece.

Regarding the profiles of DOC (Fig. 4), one could observe that since high values are found in deeper layers of all stations, it seems that the water column is strongly influenced by the municipal waste outflows that spread through cyclonic currents that dominate the area [42]. Common sense is that the highest values of DOC are found near the sea bottom of our stations. This is an additional evidence of the impact by the WWTP of Psitalia. Since the pipeline outflows pretreated wastewaters in about 65 m depth, it seems that they are distributed in a wide area, through the dominant cyclonic current moving from south of Psitalia Island, passing next to S.5 and S.7. Thus, undoubtedly the deeper points of our stations are affected by the WWTP outfalls. In general, increased values of DOC are expected in the Saronikos Gulf, since it is a coastal area, which has been receiving increased loads of waste for a long time. Furthermore, the eutrophic conditions which characterize the gulf lead to intense primary production and subsequent release of organic compounds, increasing the DOC content notably [41].

4.2. Activity concentrations of dissolved and particulate ^{234}Th

Fig. 5 shows dissolved, particulate, total ^{234}Th and ^{238}U profiles from the winter cruise. The data can also be seen in Table 2. During winter 2007, in station S.3, the particulate ^{234}Th curve (Fig. 5) shows a reverse slope compared to the dissolved one. Nevertheless, the particulate ^{234}Th curve conforms to the total ^{234}Th fluctuation curve. The disequilibrium between total ^{234}Th and ^{238}U is larger in the bottom layer of S.3. Values found in the surface layer (0–15 m) are near equilibrium resulting in a small vertical flux. The observed sharp disequilibrium in bottom layer is likely affected by the fact that dissolved ^{234}Th can be efficiently extracted and removed by re-suspended sediments. Thus, the more dissolved thorium is reduced, as it is scavenged by suspended particles, the more particulate one is increased in S.3. In station S.5, all fractions of ^{234}Th, as well as ^{238}U are equivalent showing no degradation with depth. ^{234}Th^T/^{238}U ratio ranges between 0.3 and 0.4 depending on depth. The slight reduce of dissolved ^{234}Th can be explained possibly in terms of the notable scavenging of dissolved ^{234}Th onto particles (see J_{Th}) in 35 m depth (Fig. 5), which rises of approximately 50%. Potential remineralization or insufficient adsorption of ^{234}Th onto particles can be noted in the bottom nepheloid layer of the station by the slight increase of dissolved ^{234}Th. Finally, in station S.7 particulate ^{234}Th is homogenous throughout the water column indicating the high mixing grade of the water. On the other hand, dissolved and thus total ^{234}Th decrease rapidly with depth. This phenomenon can be explained as follows: Dissolved ^{234}Th shows high affinity for sorption onto particle in the mid-water of S.7. Increase of scavenging rate of dissolved ^{234}Th onto particles (J_{Th}) of about 80% is observed (Fig. 5). Moreover, in the middle layer of that area increased particle export flux is also found (~70%), it seems that wherever particles are available (increased TSM in this depth) ^{234}Th is

Table 2
^{238}U, particulate (P_{Th}-234), dissolved (D_{Th}-234) and total ^{234}Th (T_{Th}-234), distribution coefficient (K_d), removal rates of particulate and dissolved ^{234}Th (J_{Th} and P_{Th}), particulate and scavenging residence times (τ_p, τ_d), and particulate and removal rate constants (λ_p, λ_d) for samples collected in winter 2007 in the Eastern Saronikos Gulf, Greece

Station	Depth (m)	Salinity (psu)	U-238 (Bq m^{-3})	P_{Th}-234 (Bq m^{-3})	D_{Th}-234 (Bq m^{-3})	T_{Th}-234 (Bq m^{-3})	K_d ($\times 10^6$ cm g^{-1})
S.3	0	36.7	43.2 ± 0.9	3.8 ± 1.8	27.5 ± 1.3	31.3 ± 2.3	1.1 ± 0.5
	15	36.4	42.0 ± 0.9	1.2 ± 0.6	30.0 ± 1.2	31.2 ± 1.6	0.1 ± 0.0
	60	33.1	39.0 ± 0.8	3.3 ± 1.3	15.7 ± 1.1	19.0 ± 1.7	1.1 ± 0.5
S.5	0	38.1	44.9 ± 0.9	2.7 ± 1.4	13.2 ± 1.4	15.9 ± 1.4	0.8 ± 0.3
	35	37.9	44.6 ± 0.9	2.8 ± 0.9	12.1 ± 1.4	14.9 ± 1.5	0.8 ± 0.2
	90	38.4	45.2 ± 0.9	1.7 ± 0.9	17.0 ± 1.5	18.7 ± 1.3	0.2 ± 0.1
S.7	0	38.4	45.2 ± 0.9	1.8 ± 0.4	28.2 ± 3.9	30.0 ± 3.8	0.1 ± 0.1
	50	38.1	44.9 ± 0.9	2.9 ± 1.3	10.8 ± 1.9	13.7 ± 1.8	2.0 ± 0.9
	100	37.7	44.4 ± 0.9	2.3 ± 1.1	11.9 ± 1.4	14.2 ± 1.5	0.9 ± 0.4
	200	36.5	43.0 ± 0.9	3.6 ± 1.4	17.4 ± 1.5	21.0 ± 1.3	1.2 ± 0.5

Station	Depth integral (m)	J_{Th} (Bq m^{-2} d^{-1})	P_{Th} (Bq m^{-2} d^{-1})	τ_d (d)	τ_p (d)	λ_d ($\times 10^{-3}$ d^{-1})	λ_p ($\times 10^{-3}$ d^{-1})
S.3	0–15	6.8 ± 0.3	5.2 ± 2.6	60.5 ± 2.9	10.9 ± 5.4	17 ± 1	92 ± 46
	15–60	15.6 ± 0.6	14.1 ± 7.1	86.2 ± 3.4	3.7 ± 1.8	12 ± 1	269 ± 135
	60–65	0.7 ± 0.1	8.6 ± 4.2	23.5 ± 1.6	5.7 ± 2.8	43 ± 3	176 ± 88
S.5	0–35	30.0 ± 3.2	27.5 ± 13.6	14.5 ± 1.5	3.2 ± 1.6	69 ± 7	315 ± 33
	35–90	51.5 ± 6.0	47.0 ± 13.5	12.9 ± 1.5	3.3 ± 1.1	78 ± 9	301 ± 100
	90–97	4.1 ± 0.4	3.8 ± 1.9	21.0 ± 1.8	2.3 ± 1.1	48 ± 4	443 ± 221
S.7	0–50	24.4 ± 3.4	21.8 ± 4.6	57.8 ± 8.0	4.2 ± 0.8	17 ± 2	238 ± 48
	50–100	49.1 ± 8.6	44.9 ± 20.5	10.9 ± 1.9	3.2 ± 1.5	91 ± 16	310 ± 155
	100–200	93.5 ± 11.0	86.7 ± 43.1	12.8 ± 1.5	2.7 ± 1.3	78 ± 9	369 ± 184
	200–220	5.2 ± 0.4	4.4 ± 2.0	23.7 ± 2.0	5.7 ± 2.7	42 ± 4	176 ± 87

The uncertainties quoted for ^{234}Th activities are 1σ values derived from counting statistics, estimated by uncertainty propagation.

rapidly adsorbed onto particles, where rapidly sink to the sediments. Potential remineralization or insufficient adsorption of ^{234}Th onto particles can be noted since dissolved ^{234}Th increases near the sea bed.

4.3. Export and scavenging rates and residence times of ^{234}Th

Since the concentration of TSM in Saronikos Gulf is generally high (see Chapter 4.1), the rapid removal of ^{234}Th could lead to disequilibrium values with its parent, ^{238}U throughout the water column [43]. Analyses of particulate and dissolved ^{234}Th in the water column of the 3 stations in Saronikos Gulf indicate that there are deficiencies of ^{234}Th far from equilibrium with its parent ^{238}U, due to active scavenging on time scales of days to months (see Fig. 5).

During winter period, assuming that S.3 is a coastal station where TSM is high, we should have calculated high total ^{234}Th activity concentration, as well as high scavenging rates of dissolved ^{234}Th onto particles (J_{Th}) and particulate ^{234}Th removal rates (P_{Th}). However, the trend is the opposite, since J_{Th} and P_{Th} are in the lowest level (0.7 ± 0.1–15.6 ± 1.9 Bq m^{-2} d^{-1} and 5.2 ± 2.6–14.1 ± 7.1 Bq m^{-2} d^{-1}, respectively—Table 2). These late rates lead to the assumption that in S.3, during winter, advective processes are very important spreading the WWTP waters quickly. In S.5 generally higher fluxes are found in the water column ranging between 3.8 ± 1.9 and 47.0 ± 13.5 Bq m^{-2} d^{-1} for particles that sink to sediments and 4.1 ± 0.7 and 51.5 ± 8.6 Bq m^{-2} d^{-1} for dissolved ^{234}Th that is scavenged by particles (Table 2). Finally, in station S.7 particle export flux of ^{234}Th ranges between 4.4 ± 2.0 and 86.7 ± 43.1 Bq m^{-2} d^{-1} and ^{234}Th scavenging rate between 5.2 ± 1.0 and 93.5 ± 31.1 Bq m^{-2} d^{-1} (Table 2). Larger flux in the middle layer is observed due to boundary exchange. One of the main features of boundary exchange is the transport of dissolved and particulate species in a vice versa procedure resulting in a dynamic equilibrium between the two phases [44,45]. The fluxes are in the highest level indicating a more steady system that resembles with the open sea model. While dissolved species in open waters can be imported into nepheloid layers by particle scavenging where they can be removed to sediments, particulate species can be exported laterally into open waters by the same mechanism.

The residence times of dissolved and particulate ^{234}Th in S.3 (Table 2) indicate the following: (i) the particulate ^{234}Th residence times are the shortest at S.3 (3–10 days), (ii) they show a slight increase at 0–15 m depth. This fact, together with the simultaneous increase of ^{234}Th activity concentration just above the seabed indicates potential remineralization or insufficient adsorption of ^{234}Th onto particles. Looking at the residence times of two fractions in S.5 (Table 2), we observe that particulate ^{234}Th remains in column for about 3 days, whereas the dissolved one for 15–23 days. These values are comparable with those reported by Baskaran et al. [34] for the Gulf of Mexico or those reported by Baskaran et al. [43] for the Canada basin in the Arctic Ocean. The residence times of particulate and dissolved ^{234}Th in S.7 are between 5–7 and 10–57 days, respectively (Table 2). The notable point of that station is the fact that larger residence times are found in the surface layer. This phenomenon is probably attributed to the fact that S.7 is just next to the ship traffic of Piraeus Port affecting the surface layer by mixing, throughout the year. The high mixing grade of the water assigns a more dynamic system that delays sedimentation processes.

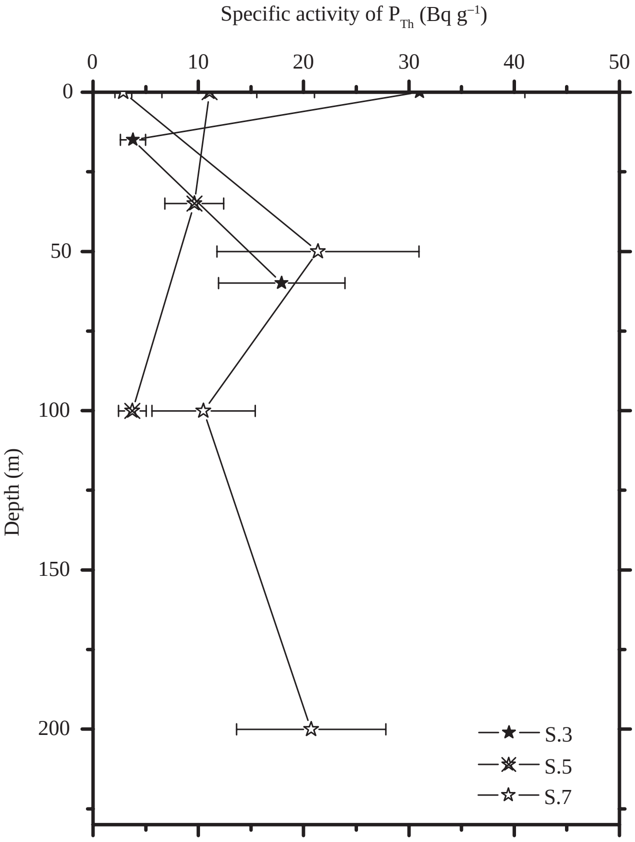

Fig. 6. Vertical profiles of specific activity of ^{234}Th activity concentrations in the three stations of sampling.

4.4. Relationship between particulate ^{234}Th and TSM

The vertical profiles of specific activity (activity concentration of particulate ^{234}Th per gram of particulate matter) of particulate ^{234}Th in the three sampling stations of the Eastern Saronikos Gulf are shown in Fig. 6. The specific activity decreases with depth in S.3, from 31 Bq g^{-1} at 0 m to 4 Bq g^{-1} at 15 m and increases to 18 Bq g^{-1} at 60 m. In S.5 specific activity continuously decreases with the depth (11–4 Bq g^{-1}). Finally, in the deepest station (S.7—220 m) the specific activity of ^{234}Th increases from 3 to 21 Bq g^{-1} at 0–50 m, decreases at 50–100 m (21–10 Bq g^{-1}) and then increases up to 21 Bq g^{-1}. Trimble and Baskaran [46] reported that the decrease of the specific activity is due to remineralization of particulate matter. The extent of remineralization seems to vary with location; however, it is intense in S.5, a station characterized by depth mixing caused by the vessels' anchors. The highest specific activity (21 Bq g^{-1}) is found at the bottom waters (200 m depth) of S.7 and this is attributed to scavenging of ^{234}Th by refractory material during vertical settling. The great variation of specific activity in the stations of sampling could be attributed to the sporadic release of particulate matter from the land and/or sediments and/or trawling activities and/or storm events, which is transported to farther distances picking up additional dissolved ^{234}Th from the water column [43].

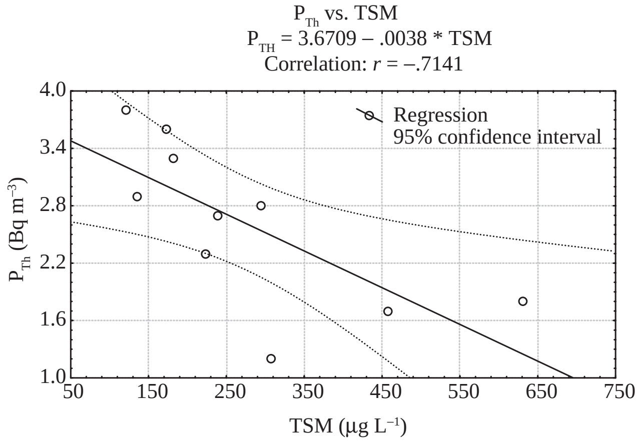

Fig. 7. Particulate ^{234}Th activity concentrations (P_{Th}) plotted against total suspended matter (TSM) concentrations.

The activity concentrations of particulate ^{234}Th are plotted against TSM in Fig. 7. Thus, particulate ^{234}Th is well correlated ($R = -0.7141$, $P < 0.001$) with TSM showing that the removal of particulate ^{234}Th is primarily controlled by the particle concentration. However, since that correlation curve should tend to straight line, one can note that in the Eastern Saronikos Gulf marine environment the assumption of negligible advection and diffusion processes might not be fulfilled and this indicates that other processes could be dominant.

4.5. Distribution coefficient K_d

The distribution coefficient of Th, K_d ($K_d = A_p/[A_d \times \text{TSM}]$) represents its equilibrium distribution and more specifically the observed solid/solution partitioning in the water column [47]. The particle/water partitioning coefficient of ^{234}Th in the three sampling stations varies from 0.1 ± 0.0 to $2.0 \pm 0.9 \times 10^6$ cm^3 g^{-1} (Table 2). These values are comparable to those reported for other areas, world widely. Specifically, Trimble and Baskaran [46] reported mean K_d values 0.5×10^6 cm^3 g^{-1} in the Canada Basin, Cochran et al. [48] mean value of 0.4×10^6 cm^3 g^{-1} in Greenland, Moran and Smith [49] mean value of 2.6×10^6 cm^3 g^{-1} in Beaufort Sea and Baskaran et al. [43] a higher mean value of 4.0×10^6 cm^3 g^{-1} in Western Arctic. The variation of the K_d partitioning coefficient is strongly influenced by the fact that Saronikos Gulf is an eutrophic marine environment and the present pigments are the major factor of thorium partitioning in the area.

4.6. Relationship between DOC and dissolved ^{234}Th activity concentration

Since up to 50% of DOC exists in the form of colloidal particles [50], and significant amounts of ^{234}Th have been found to be associated with colloids [51–53], one might expect some relationship between the dissolved ^{234}Th concentration and DOC. This is not confirmed by the data, which show weak linear correlation between dissolved ^{234}Th and DOC concentrations in the three stations (Fig. 8). However, significant correlation is observed, if one excludes station S.3 ($R = 0.8307$, $P < 0.001$). As mentioned previously, S.3 is located near the outflow of the WWTP of Psitalia and this fact introduces the major source of organics in the area. Thus, in this area dissolved ^{234}Th distribution is not controlled by DOC. On the other hand, the correlation found in S.5 and S.7 may indicate that, at higher DOC concentrations, more colloids are available for the removal of thorium by the coagulation of colloids. The higher the fraction of ^{234}Th associated with colloids is, the more intense colloidal pumping and thorium scavenging [52,55] associated with dissolved organic matter (DOM) occurs.

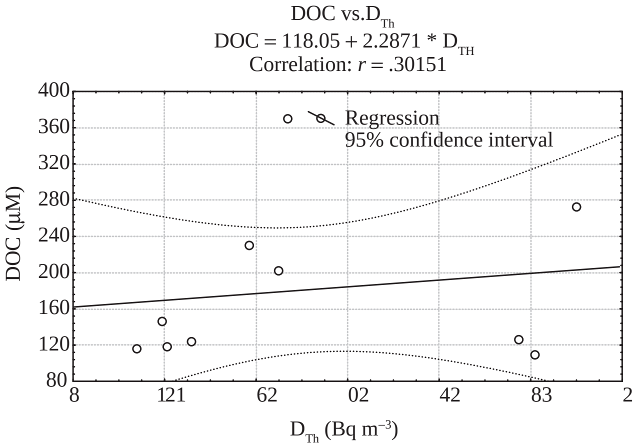

Fig. 8. Dissolved organic carbon (DOC) concentrations plotted against dissolved ^{234}Th (D_{Th}) concentrations.

5. Conclusions

In the present study the role of particles (>0.6 µm) and selected biomarkers in controlling the removal of particle-reactive ^{234}Th from waters is investigated. Moreover, the residence times of dissolved and particulate ^{234}Th are also determined. Finally, an attempt is made to investigate if there is any relationship between (i) particulate ^{234}Th and TSM as an indication of the scavenging and removal of ^{234}Th in areas characterized by enhanced TSM concentration and (ii) DOC and dissolved ^{234}Th concentrations as an indication of the effect of binding of ^{234}Th by dissolved organic ligands. The significant findings of the present study are:

(1) The marine environment of the Eastern Saronikos Gulf is strongly influenced by the discharges of municipal wastes by the WWTP of Psitalia. This is confirmed by the environmental parameters showing stratification in S.3 during winter and the elevated TSM and DOC concentrations.

(2) There is a strong disequilibrium between total ^{234}Th and ^{238}U in the water column of our stations during winter and this is attributed to lateral exchange of dissolved and particulate species in continental margin waters. The activities of two radionuclides tend to equilibrium only in the surface point of S.3, leading to slow export flux of particulate ^{234}Th. No resuspension processes can be concluded, since the ratio $^{234}\text{Th}^{\text{T}}/^{238}\text{U}$ is less than 1.

(3) The correlation observed (almost 1:1) between dissolved ^{234}Th scavenging rates onto particle (J(Th)) and particle export fluxes to sediments (P(Th)) are in agreement with the predictions of the colloidal pumping model of Honeyman and Santschi [55]. This model suggests that truly dissolved elements are converted to a filterable particle fraction via colloidal intermediates, by (i) rapid equilibration of dissolved metal species with particle surface sites, both on colloids and in the filterable-particle fractions and (ii) slower aggregation of colloids with larger particles.

(4) Regarding to the residence times of particulate and dissolved ^{234}Th, they present comparable values in all stations, except S.3. In this station, values for dissolved ^{234}Th are significantly higher due to the presence of an additional source of particles (WWTP of Psitalia).

(5) Remineralization or insufficient adsorption of ^{234}Th onto particles is likely dominant in the nepheloid layer of S.5, since TSM and dissolved ^{234}Th concentrations increase and specific activity of ^{234}Th decrease.

(6) Significant correlation between TSM and particulate ^{234}Th ($R = -0.7141$) is observed indicating that the removal of particulate ^{234}Th is controlled by the suspended particles. Also distribution coefficient of ^{234}Th is similar to those reported in the relevant literature.

(7) There is a significant correlation between dissolved ^{234}Th and DOC concentrations ($R = 0.8307$) in S.5 and S.7 suggesting the possibility that the major carrier phase for thorium cycling is DOC of which a significant fraction is in the colloidal range. Thus, at higher DOC concentrations, more colloids can be removed by coagulation, resulting in lower dissolved ^{234}Th concentrations.

Acknowledgements

The authors of this paper would like to thank the Head of the Environmental Radioactivity Laboratory (NCSR ''Demokritos''), Dr P. Kritidis and the permanent staff, Mrs Ch. Psomiadou, Mrs A. Zafiropoulou and Mr St. Michaleas for their support, as well as the crew of the vessel used for the sampling.

References

[1] S.G. Bhat, S. Krishnaswamy, D. Lal, Rama and W.S. Moore, Earth Planet. Sci. Lett., 5 (1969) 483-491.
[2] E.D. Goldberg, J. Geol., 62 (1954) 249-265.
[3] E. Matsumoto, Geochim. Cosmochim. Acta, 39 (1975) 205-212.
[4] J.K. Cochran and P. Masque, Rev. Mineral. Geochem., 52 (2003) 461-492.
[5] K.H. Coale and K.W. Bruland, Limnol. Oceanogr., 30 (1985) 22-33.
[6] K.H. Coale and K.W. Bruland, Limnol. Oceanogr., 32 (1987) 189-200.
[7] N. Savoye, C. Benitez-Nelson, A.B. Burd, J.K. Cochran, M. Charette, K.O. Buesseler, G. Jackson, M. Roy-Barman, S. Schmidt and M. Elskens, Mar. Chem., 100 (2006) 234-249.
[8] K.O. Buesseler, C.R. Benitez-Nelson, S.B. Moran, A.B. Burd, M. Charette, J.K. Cochran, L. Coppola, N.S. Fisher, S.W. Fowler, W.D. Gardner, L.D. Guo, O. Gustafsson, C. Lamborg, P. Masque, J.C. Miquel, U. Passow, P.H. Santschi, N. Savoye, G. Stewart and T. Trull, Mar. Chem., 100 (2006) 213-233.
[9] M. Baskaran and P.W. Swarzenski, Mar. Chem, 104 (2007) 27-42.
[10] N. Friligos, Mar. Poll. Bull., 13(1982) 154-158.
[11] E. Voutsinou-Taliadouri, Mar. Poll. Bull., 12 (1981) 163-168.
[12] M. Dassenakis, M. Scoullos, K. Rapti, A. Pavlidou, D. Tsorova, V. Paraskevopoulou, E. Rozi, A. Stamateli and M. Siganos, Global Nest Int. J., 5 (2004) 133-143.
[13] W.R. Simpson (Eds), Deep sea in situ particle samplers (using the Mark III centrifugal pump. Operating Manual, Challenger Oceanic Systems and Services, UK, 1997.
[14] D.R. Mann, L.D. Surprenant and S.A. Casso, Nucl. Instrum. Methods Phys. Res., Sect. A, 223 (1984) 235-238.
[15] H.D. Livingston and J.K. Cochran, J. Radioanal. Nucl. Chem. Art., 115 (1987) 299-308.
[16] P. Roos, E. Holm and R.B.R. Persson, Nucl. Instrum. Methods Phys. Res., Sect. A, 339 (1994) 282-286.
[17] J.H. Chen, R.L. Edwards and G.J. Wasserburg, Earth Planet. Sci. Lett., 80 (1986) 241-251.
[18] S. Schmidt and J.L. Reyss, Comptes Rendus de l'Academie de Science de Paris Serie II, 312 (1991) 479-484.
[19] D. Delanghe, E. Bard and B. Hamelin, Mar. Chem., 80 (2002) 79-93.
[20] J. Carroll and W.S. Moore, Geochim. Cosmochim. Acta, 57 (1993) 4987-4995.
[21] M. Kersten, S. Thomsen, W. Priebsch and C.-D. Garbe-Schonberg, Appl. Geochem., 13 (1998) 339-347.
[22] B.A. McKee, D.J. DeMaster and C.A. Nittrouer, Geochim. Cosmochim. Acta, 51 (1987) 2779-2786.
[23] Y. Sigimura and Y. Suzuki, Mar. Chem., 24 (1988) 105-131.
[24] G. Cauwet, Mar. Chem., 47 (1994) 55-64.
[25] M. Frignani, T. Courp, J.K. Cochran, D. Hirschberg and L. Vitoria i Codina, Cont. Shelf Res., 22 (2002) 2175-2190.
[26] J.M. Foster and G.B. Shimmield, Deep Sea Res. II, 49 (2002) 2965-2977.
[27] S.B. Moran and K.O. Buesseler, J. Mar. Res., 51 (1993) 893-922.
[28] C.L. Wei and J.W. Murray, Limnol. Oceanogr., 37 (1992) 296-314.
[29] O. Radakovitch, M. Frignani, S. Giuliani and R. Montanari, Estuarine Coastal Shelf Sci., 58 (2003) 813-824.
[30] M.P. Bacon, J.K. Cochran, D. Hirschberg, T.R. Hammar and A.P. Fleer, Deep Sea Res. II, 43 (1996) 1133-1153.
[31] K.O. Buesseler, J.A. Andrews, M.C. Hartman, R. Belastock and F. Chai, Deep Sea Res. II, 42 (1995) 777-804.
[32] C.R. Benitez-Nelson, K.O. Buesseler and G. Crossin, Cont. Shelf Res., 20 (2000) 707-736.
[33] O. Gustafsson, K.O. Buesseler, W.R. Geyer, S.B. Moran and P.M. Gschwend, Cont. Shelf Res., 18 (1998) 805-829.
[34] M. Baskaran, P.H. Santschi, L. Guo, T.S. Bianchi and C. Lambert, Cont. Shelf Res., 16 (1996) 353-380.
[35] E. Krasakopoulou and A.P. Karageorgis, Geo-Mar. Lett., 25 (2005) 343-359.
[36] G.K.P. Muir, J.M. Pates, A.P. Karageorgis, and H. Kaberi, Cont. Shelf Res., 25 (2005) 2476-2490.
[37] G. Cauwet, F. Gadel, M.M. de Souza Sierra, O. Donald and M. Ewald, Cont. Shelf Res., 10 (1990) 1025-1037.
[38] G. Cauwet, A. Miller, S. Brasse, G. Fengler, R.F.C. Mantoura and A. Spitzy, Deep Sea Res. II, 44 (1997) 769-779.
[39] G. Copin – Montegut and B. Avril, Deep-Sea Res. I, 40 (1993) 1963-1972.

[40] A.E.J. Miller, R.F.C. Mantoura and M.R. Preston, Mar. Chem., 41 (1993) 215-221.

[41] C. Zeri and E. Krasakopoulou, In: Proceedings of the 7th International Conference on Environmental Science and Technology, Ermoupolis, Syros Isl., Greece, 2001.

[42] A. Laskaratos and N. Kaltsounidis, Final report on the study of the hydrodynamics and pollution by the effluents of Athens. University of Athens, Athens, Greece, 1987.

[43] M. Baskaran, P.W. Swarzenski and D. Porcelli, Deep Sea Res. I, 50 (2003) 1353-1373.

[44] P.H. Santschi, U.P. Nyffeler, Y.-H. Li, P. O'Hara and P.G. Sly (Eds), Springer Verlag, Berlin, 1986.

[45] H.H. Jannasch, B.D. Honeyman, L.S. Balistrieri and J.W. Murray, Geochim. Cosmochim. Acta, 52 (1988) 567-577.

[46] S.M. Trimble and M. Baskaran, Mar. Chem., 96 (2005) 1-19.

[47] B.D. Honeyman, L.S. Balistrieri and J.W. Murray, Deep Sea Res., 35 (1988) 227-246.

[48] J.K. Cochran, C. Barnes, D. Achman and D.J. Hirschberg, J. Geophys. Res., 100 (1995) 4399-4410.

[49] S.B. Moran and J.N. Smith, Cont. Shelf Res., 20 (2000) 153-167.

[50] L. Guo, C.H. Coleman and P.H. Santschi, Mar. Chem., 45 (1994) 105-119.

[51] M. Baskaran and P. H. Santschi, Mar. Chem., 43 (1993) 95-114.

[52] M. Baskaran, P.H. Santschi, G. Benoit and B.D. Honeyman, Geochim. Cosmochim. Acta, 56 (1992) 3375-3388.

[53] B. Moran and K. Buesseler, Nature, 359 (1992) 221-223.

[54] P.H. Santschi, L. Guo, M. Baskaran, S. Trumbore, J. Southon, T.S. Bianchi, B.D. Honeyman and L. Cifuentes, Geochim. Cosmochim. Acta, 59 (1995) 625-631.

[55] B.D. Honeyman and P.H. Santschi, J. Mar. Res., 47 (1989) 951-992.